International Database of Neutron Monitor Measurements: Development and Applications

D. SAPUNDJIEV, PHD • T. VERHULST, PHD • S. STANKOV, PHD

20.1 INTRODUCTION

Cosmic rays are the particles and the radiation present in the interstellar space originating from natural cosmological processes related to the lifecycle of stellar objects, including the Sun. The basic characteristics of cosmic rays are their composition and energies. Cosmic rays arriving in the interplanetary space are called primary or galactic cosmic rays (GCRs). They include also particles originating from the Sun – solar wind – which have greater intensity and lower energies. The latter are named solar cosmic rays (SCRs). The SCR intensity and energy distribution are related to the primary solar activity variations (solar cycles) and the random activity known as space weather. Because of their greater intensity, the SCRs alter (modulate) the intensity and energy spectrum of the cosmic rays that enter the solar system. When the Sun is active, fewer cosmic rays reach the Earth than during times when the Sun is quiet. As a result, the cosmic rays follows an 11-year cycle like the Sun's activity level but in the opposite direction: higher solar activity corresponds to lower intensity of cosmic rays, and vice versa (Fig. 20.1). Monitoring of this modulation is used for analysis of the interplanetary medium and the solar activity and its effects on the Earth.

On entering the atmosphere, cosmic rays interact with its constituents by a series of cascade reactions, resulting in a large number of secondary particles. Measurements showed that neutrons and protons constitute the largest fraction of the secondary particles at sea level. Thus, to be able to constantly monitor these secondary particles on the ground, a reliable instrument was developed in the 1950s – the so-called neutron monitor (Simpson, 2000). The design of the neutron monitor consists of four main parts (Fig. 20.2): a large proportional counter (tube) filled with boron trifluoride ($^{10}BF_3$), a cylindrical moderator from hydrogen-rich material, a high-atomic number neutron producer made of lead (Pb), and an outer box of hydrogen-rich material – reflector (Hatton and Carimichael, 1964). The protons and the neutrons produced in the atmospheric interactions produce an additional number of neutrons in the lead producer. The neutrons are slowed down (moderated) in the hydrogen-rich cylinder inside the producer in order to increase the detection probability in the detector. The surrounding reflector is used to moderate and reflect neutrons coming from other sources than the cosmic rays (Stoker, 2009).

Neutron monitors have been in continuous operation since the late 1950s. It was soon realized that the scientific value of the data will be much greater if there are multiple stations positioned at different geomagnetic locations. The results from several latitude surveys showed the dependence of neutron monitor measurements on geomagnetic latitude. A practical measure to compare measurements made at different locations on Earth is the geomagnetic cutoff rigidity. Several cosmic rays stations were operating neutron monitors with comparable design, which made possible the use of the geomagnetic field to analyze the primary cosmic ray properties (Simpson et al., 1953). Initially, the data from the available stations were collected in various World Data Centers (WDCs). The first network of operating neutron monitors was initiated during the international geophysical year (1957). During these periods data accessibility and dissemination was tedious and slow, which hindered analysis and research.

Why does monitoring the cosmic rays matter? Cosmic rays have a substantial impact on the Earth's atmosphere by the secondary particles they produce when colliding with atmospheric atoms and by the ionization of atmospheric atoms. Fast charged particles are a source of irradiation, as are X-rays, and therefore can be hazardous. While there seems to be little effect on the ground, aircraft and spacecraft crews are less protected by the atmosphere. As a result, long-time exposure of pilots and cabin crew, especially on transpolar routes, increases the possibility of adverse effects of the cosmic

Knowledge Discovery in Big Data from Astronomy and Earth Observation. https://doi.org/10.1016/B978-0-12-819154-5.00032-1

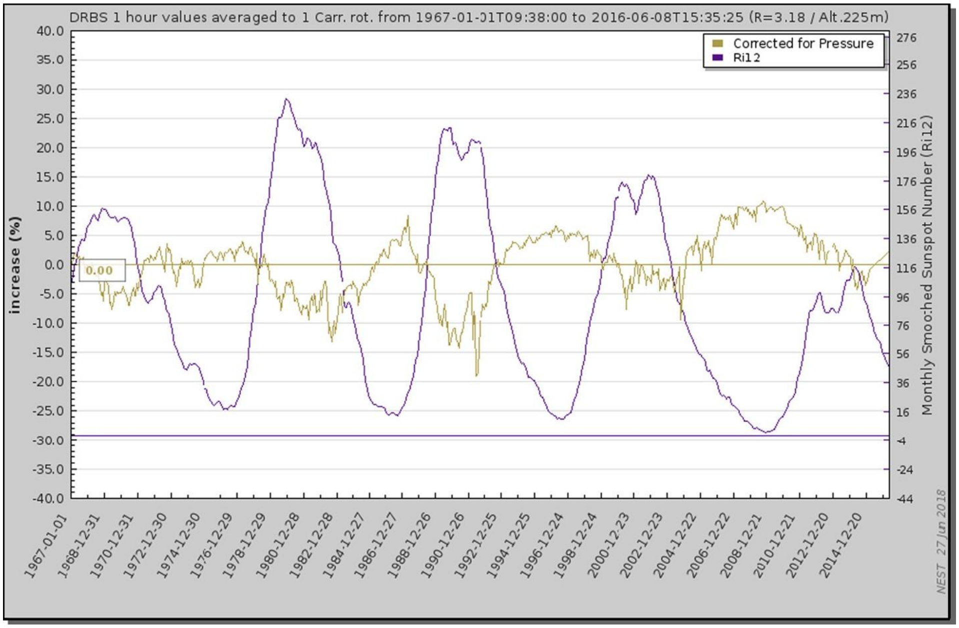

FIG. 20.1 Solar modulation of the cosmic ray intensity based on long-time measurements from the neutron monitor in Dourbes, Belgium (image courtesy of NMDB; smoothed sunspot numbers and monthly sunspot numbers are provided by the Solar Influences Data Analysis Center [SIDC], Royal Observatory of Belgium).

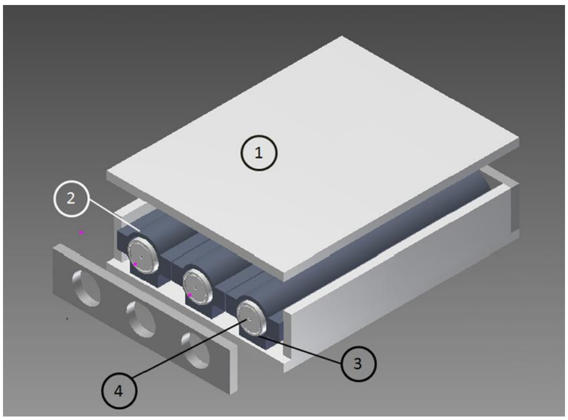

FIG. 20.2 Schematic of a three-tube neutron monitor design (3-NM64): moderator tubes (3) housing the proportional detectors (4), producer (2), and reflector (1).

radiation. Also, short-time increased radiation during strong solar energetic particle (SEP) events can have adverse effects on passengers and avionics. High-frequency (HF) radio communications in the polar regions are also affected by polar cap absorption events due to SEP events. In addition to the adverse effects of the cosmic radiation on astronauts, there is also a potential risk for damage of spacecraft equipment. As the modern society relies more and more on aircraft/space travel, cosmic radiation effects need to be monitored and investigated.

20.2 THE NEUTRON MONITOR DATABASE (NMDB)

20.2.1 The Need for NMDB

The increasing space weather awareness posed more rigorous demands on the data quality, accessibility, and real-time availability. The strong dependence of neutron monitor count rate on the solar cycle and solar activity together with its simple design and low maintenance costs rendered the neutron monitor an important tool in space weather research and monitoring. In 2007 several European and non-European institutions decided to systematize, optimize, and provide reliable data in real-time from the operating stations worldwide and also to provide historical data of ground-based cosmic ray stations continuously measuring the neutron intensity. The idea evolved into a project that was funded for 2 years (2008–2009) by the European Union's Seventh Framework Programme (FP7) for Research and Techno-

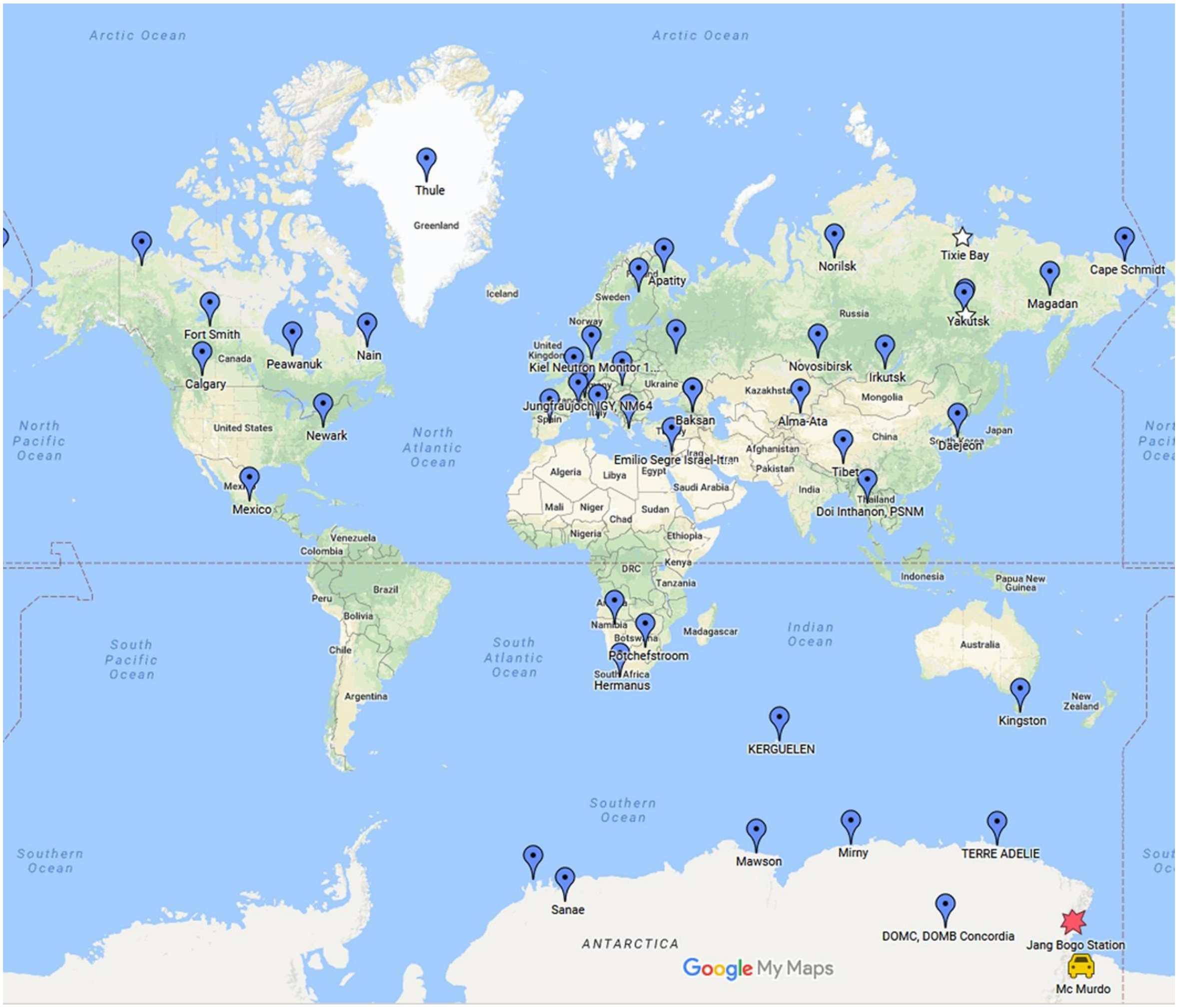

FIG. 20.3 A global map showing the locations of the neutron monitor stations (image courtesy of NMDB).

logical Development (Capacities) (Steigies et al., 2009). The neutron monitor database (NMDB) was thus created[1] and by the end of 2009 there were already 14 stations providing data in real-time.

The main objectives of the project were to create an interactive database that is capable to:

- provide data in standard format,
- provide high-resolution data,
- offer real-time data with a targeted delay of less than 5 min,
- offer easy access to the data,
- provide design for modern registration systems,
- develop online applications using the neutron monitor data.

The project started by first collecting hourly data in the WDC format (now World Data System under the International Council for Science).[2] At that time there were no real-time or high-resolution data, which are required for space weather applications. A year later, in 2008, the NMDB commenced operation by collecting data in near-real-time from several stations. Later on, more and more institutions worldwide have joined the NMDB consortium. As of 2019, the NMDB collects data from more than 60 cosmic ray stations (Fig. 20.3).

[1] www.nmdb.eu.

[2] www.icsu-wds.org.

About half of them (Table 20.1) are providing data in real-time in the rigidity range from 0 at the poles to 15 GV at the geomagnetic equator utilizing the entire GMF for analysis and observations.

20.2.2 The NMDB Database

The NMDB is a centralized state-of-the-art database with distributed mirrors. At the time of writing, it has two master file servers – an active (db01) and a passive database server (db02). Each member of the NMDB consortium provides its data to the active master server. The data are then synchronized with the passive master server. The master server is also responsible for disseminating the data to a mirror server (db04), which has the objective to distribute the data to the three external mirrors of the NMDB, located in Moscow (db10), Athens (db20), and Oulu (db30). To provide sufficient data redundancy each mirror has a complete copy of the NMDB. The fan-out server (db04) to the slave servers: db03 for external users, db05 (a slave server at the ET), and a third slave server, db06, at the neutron monitor. The external users can have data access via the slave db03 in read-only mode. The structure of the NMDB hardware is illustrated in Fig. 20.4.

The data are arranged in several tables. The first table contains detailed information about each station contributing data to the NMDB (Fig. 20.5). This information, coordinates, geomagnetic cutoff, altitude, detector type, building materials, and surrounding materials, etc., is required in order to use the station data for analysis of the cosmic ray properties and correct evaluation of the intensity measurements. Among the most important parameters contained in this table are the average count per solar minimum and maximum, which are used by the NMDB software to calculate the relative intensity change of the station.

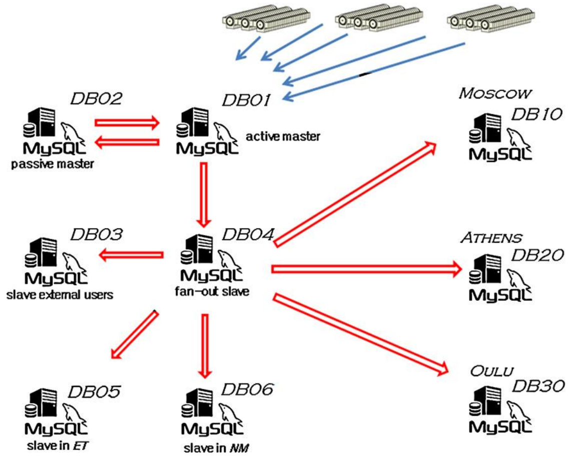

FIG. 20.4 A schematic view of the NMDB structure and data exchange (Steigies, 2016).

```
## ---------------------------------------------------------------------------
##describe station_information;
##+-----------------------------+---------------+------+-----+---------+----------------+
##| Field                       | Type          | Null | Key | Default | Extra          |
##+-----------------------------+---------------+------+-----+---------+----------------+
##| ID                          | bigint(20)    | NO   | PRI | NULL    | auto_increment |
##| station_full_name           | varchar(100)  | NO   |     |         |                |
##| station_short_name          | varchar(20)   | NO   |     |         |                |
##| start_date_time             | date          | NO   |     | NULL    |                |
##| end_date_time               | date          | YES  |     | NULL    |                |
##| head_organization           | varchar(1000) | NO   |     |         |                |
##| principal_investigator      | varchar(200)  | NO   |     |         |                |
##| contact_person              | varchar(200)  | NO   |     |         |                |
##| latitude_deg                | float         | NO   |     | 0       |                |
##| longitude_deg               | float         | NO   |     | 0       |                |
##| altitude_m_asl              | float         | NO   |     | 0       |                |
##| geomag_cutoff_GV            | float         | NO   |     | 0       |                |
##| avg_count_per_sec_solar_min | float         | NO   |     | 0       |                |
##| avg_count_per_sec_solar_max | float         | NO   |     | 0       |                |
##| ref_pressure_mbar           | float         | NO   |     | 0       |                |
##| barometric_coefficient      | float         | NO   |     | 0       |                |
##| detector_housing            | varchar(1000) | YES  |     |         |                |
##| counter_tube_type           | varchar(100)  | NO   |     |         |                |
##| counter_tube_num            | int(11)       | NO   |     | 1       |                |
##| detector_info               | varchar(1000) | NO   |     |         |                |
##| pressure_sensor             | varchar(1000) | NO   |     |         |                |
##| clock_info                  | varchar(200)  | NO   |     |         |                |
##| additional_station_info     | varchar(2000) | NO   |     |         |                |
##+-----------------------------+---------------+------+-----+---------+----------------+
```

FIG. 20.5 Table structure containing comprehensive data for every station providing measurements to the NMDB. This information is a prerequisite for correct use of the data for analysis and calculations (image courtesy of NMDB).

20.2.3 Data Contribution and Dissemination

For every station there are three basic tables containing the measured data: the original data table, the revised data table, and the hourly data table. The tables' structure is outlined in Table 20.2.

An additional table per station contains metadata like the timestamp of the first and the last record, the number of records, and the time elapsed from the last recorded measurement. Table 20.3 is used for diagnostics of the health of the individual contributing station and the database as a whole.

Most of the NMDB data providers are performing measurements at 1 min resolution. The raw data consist of the count rate of every detector tube (nine for the DRBS neutron monitor) and the atmospheric pressure measured at the location of the neutron monitor. The raw data are often subjected to an automatic quality check to filter out (remove) noisy tube measurements, and prepare the data to be sent to the NMDB (Sapundjiev et al., 2014, 2016a, 2016b). The data format at this stage consists of the date and time, the pressure (mbar), total counts (i.e., the sum of the individual detector tubes), the total counts corrected for pressure, and the relative intensity change. A portion of the 1 minute data file from the Dourbes neutron monitor is given in Table 20.3.

Every minute the new data are read from this file and sent to the NMDB active master server. Before the NMDB database is populated, a standard quality check (to detect and remove spikes, check pressure values,

TABLE 20.1
NM64-type neutron monitor stations providing data to the NMDB (data courtesy of NMDB).

Station	Rigidity (GV)	Altitude (m)	Number of detectors	Latitude (°)	Longitude (°)
TERA	0.01	32	9	−66.65	140
INVK	0.30	21	18	−68.35	−133.72
THUL	0.30	26	9	76.5	68.7
JBGO	0.30	30	5	−74.6	164.2
TXBY	0.48	0	18	71.36	128.54
NRLK	0.63	0	18	69.26	88.05
APTY	0.65	181	18	67.57	33.4
SNAE	0.73	856	6	−71.667	−2.85
OULU	0.81	15	9	65.05	25.47
KERG	1.14	33	19	−49.35	70.25
YKTK	1.65	105	18	62.01	129.43
MGDN	2.09	220	18	60.04	151.05
KIEL	2.36	54	18	54.3399	10.1199
MOSC	2.43	200	24	55.47	37.32
MCRL	2.46	2000	6	55.47	37.32
NVBK	2.91	163	24	54.48	83
DRBS	3.18	225	9	50.1	4.6
IRKT	3.64	475	18	52.47	104.03
IRK2	3.64	2000	12	52.37	100.55
IRK3	3.64	3000	6	51.29	100.55
LMKS	3.84	263	8	49.2	20.22
JUNG1	4.49	3475	3	46.55	7.98
HRMS	4.58	26	12	−34.43	19.23
BKSN	5.70	1700	6	43.28	42.69
BURE	5.00	2555	3	44.633889	5.907222
BKSN	5.70	1700	6	43.28	42.69
ROME	6.27	0	20	41.86	12.47
PTFM	6.94	1351	12	−26.68	27.09
CALM	6.95	708	15	40.559167	−3.1625
NANM	7.10	2000	18	40.3667	44.25
MXCO	8.28	2274	6	19.33	−260.82
ATHN	8.53	260	6	37.97	23.78
TSMB	9.15	1210	18	−19.2	17.58
DJON	11.22	200	18	36.24	127.22
PSNM	16.80	2565	18	18.59	98.49

TABLE 20.2
Data structure of a single measurement: original, revised, and hourly data.

	Original data	Revised data	Hourly data
start_date_time	yes	yes	yes
length_time_interval_s	yes	yes	
uncorrected	yes	yes	yes
corr_for_efficiency	yes	yes	yes
corr_for_pressure	yes	yes	yes
pressure_mbar	yes	yes	yes
version		yes	

TABLE 20.3
An example of the original minute data measurements from the Dourbes Neutron Monitor.

Date	Time, UTC	p (mbar)	Raw counts	Corrected counts	Relative
...	...	...	...	...	...
30/06/2016	00:00:00	986.65	6214.65	6217	−10.1446
30/06/2016	01:00:00	986.67	6373.02	6377	−7.84114
30/06/2016	02:00:00	986.71	6309.16	6315	−8.7377
...	...	...	...	...	...

etc.) is executed. Following this the data are synchronized with the passive master server and then sent to the slaves and the mirrors (Fig. 20.4).

A second set of data is sent in a similar way to the NMDB. This is the hourly average measurements. An hour average is calculated only if there are at least 75% of the measurements during this hour (e.g., 45 min). The files have the same data format with the difference that the measurement data are averaged over an hour. This allows faster data access and display for data requests over large time intervals. The hourly data are typically transferred at 15 min past an hour. For the stations that have performed analysis of their detector and have calculated the detector efficiency, their data are corrected for efficiency and populated in the corresponding table.

The minute and hourly data just described are corrected and sent to the NMDB automatically. Despite data quality control, it is not 100% immune to errors coming from combinations of noisy tubes that could not be filtered out by the correction algorithms (this is the case when more than half of the tubes are producing noisy and erroneous data). For this purpose every station PI is encouraged to manually revise the minute and hourly data and send it to the corresponding data tables. The easiest way to access the data from the NMDB is to use the NMDB Event Search Tool (NEST), developed and maintained by the Paris Observatory. It is implemented as a web interface on the NMDB web site offering a large number of possibilities for data retrieval and display (Fig. 20.6). The color code shows the stations which are currently online. NEST provides a quick access to the entire set of recognized Ground Level Enhancement (GLE) and Forbush decrease (FD) events. It also offers the possibility to request historical data for all of the participating cosmic rays stations. NEST is optimized for fast data delivery depending on the requested time interval. It offers the possibilities to retrieve the data in an ASCII format and/or as a plot. Useful additional information is available, like the Kp index, the proton flux from the GOES satellite, the sunspot number, and numerous options concerning the data that are requested (raw counts, pressure, and/or efficiency corrected). For advanced users and developers of NMDB-tools, e.g. real-time applications using the data, a read-only account to the database can be set. The

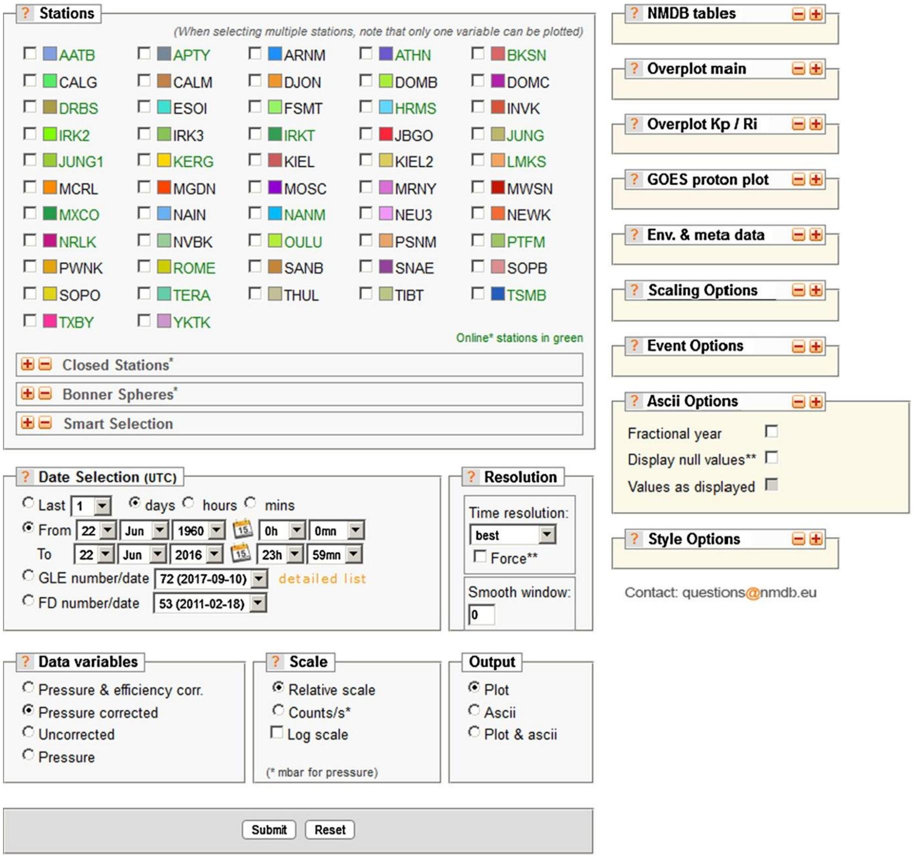

FIG. 20.6 A screen capture of the NMDB Event Search Tool (NEST) – the online interface for data plotting and retrieval developed by the Paris Observatory (image courtesy of NMDB).

web site interface allows a quick check of the cosmic ray intensity worldwide via the Cosmic Rays Now plot provided by NEST. The health of the monitors and the data quality can be checked via the NMDB status tool available from the web site interface. This tool provides useful information for the stations currently online and the data they are providing. The tool has several options to choose from (cf. Fig. 20.7).

20.3 APPLICATIONS

The two principal user groups of the NMDB data are the astrophysicists and space weather forecasters. The former are using the long datasets of historic data in the database to search for periodicities and quasiperiodicities in the intensity of the GCRs (Kudela et al., 2009). The latter use high-resolution real-time NMDB data to develop several research applications for prediction of space weather events (Mavromichalaki et al., 2011). Due to the high energy and stability of the GCR component and the nature of their interaction with solar wind, observations of cosmic ray anisotropies by the global network of neutron monitors can serve as precursors for energetic solar particles directed towards the Earth (Belov et al., 2001, 2017; Dorman et al., 2004). At present the NMDB offers several applications (some of which are provided by external research institutions), such as daily cosmic ray variations, ionization rates and atmospheric dose rates, GLE spectrum, and GLE alert.

20.3.1 Ground Level Enhancements (GLEs) – Detection and Characterization

Thanks to the reliable measurements and stable performance of the neutron monitors, the strong correlation between the GCR flux and the solar activity could be observed (Fig. 20.1). The great number of stations in

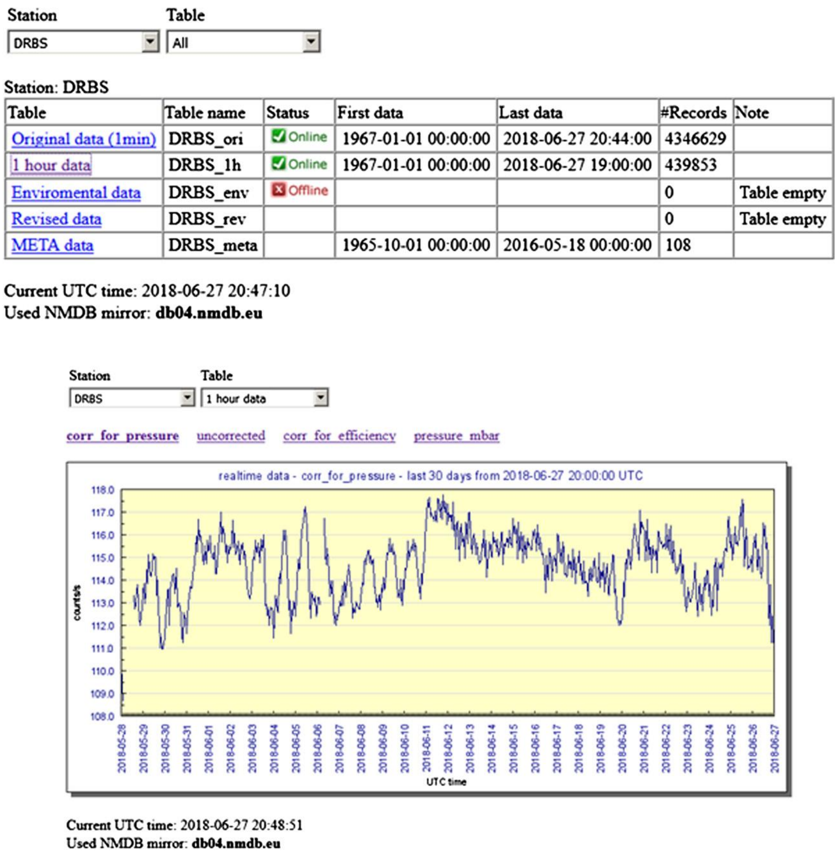

Table	Table name	Status	First data	Last data	#Records	Note
Original data (1min)	DRBS_ori	Online	1967-01-01 00:00:00	2018-06-27 20:44:00	4346629	
1 hour data	DRBS_1h	Online	1967-01-01 00:00:00	2018-06-27 19:00:00	439853	
Enviromental data	DRBS_env	Offline			0	Table empty
Revised data	DRBS_rev				0	Table empty
META data	DRBS_meta		1965-10-01 00:00:00	2016-05-18 00:00:00	108	

FIG. 20.7 Quick check tool using the metadata. (Top) Quick diagnostics of the data and availability of the Dourbes neutron monitor. (Bottom) Hourly data (as selected from the table above) (image courtesy of NMDB).

the NMDB allows for mapping of the random events within the geomagnetic field. During high solar activity, the Sun is capable of accelerating particles to very high energies, as noticed by ground level observations. These events are registered by the neutron monitors as a GLE or a substantial decrease in the count rate, known as FD (Forbush, 1946). The observed variations in the count rate of the neutron monitors are still a subject of scientific research. The NEST has a quick access option to select and display any of the recognized GLE events as well as quick access shortcuts to the last two or three GLE events (Figs. 20.8 and 20.9). From Fig. 20.8 we can note that the relative increase in the neutron monitor count rate depends strongly on the geomagnetic position of the station for comparable neutron monitor designs (both Dourbes and Oulu operate a nine-tube neutron monitor, 9-NM64, while Rome is running a 20-tube monitor, 20-NM64).

The relative increase in the count rate of a neutron monitor is a function of the geomagnetic rigidity and the atmospheric depth. At a given time instant the relative count rate increase is related to the primary cosmic ray spectrum via the specific yield of the neutron monitor for a given intensity of the secondary particles. Mathematically this is accounted for by the neutron monitor yield function. Three methods for determination of the yield function are utilized (Clem and Dorman, 2000): theoretical calculation, Monte Carlo simulations of particles transports (Wainio et al., 1968; Mishev et al., 2013), and parametrization of experimental latitude surveys (Treiman, 1952; Lockwood and Webber, 1967; Caballero-Lopez and Moraal, 2012), or sometimes combinations of those (Flückiger et al., 2008). The yield function depends on the primary particle type, its direction, and the design of the neutron monitor. The

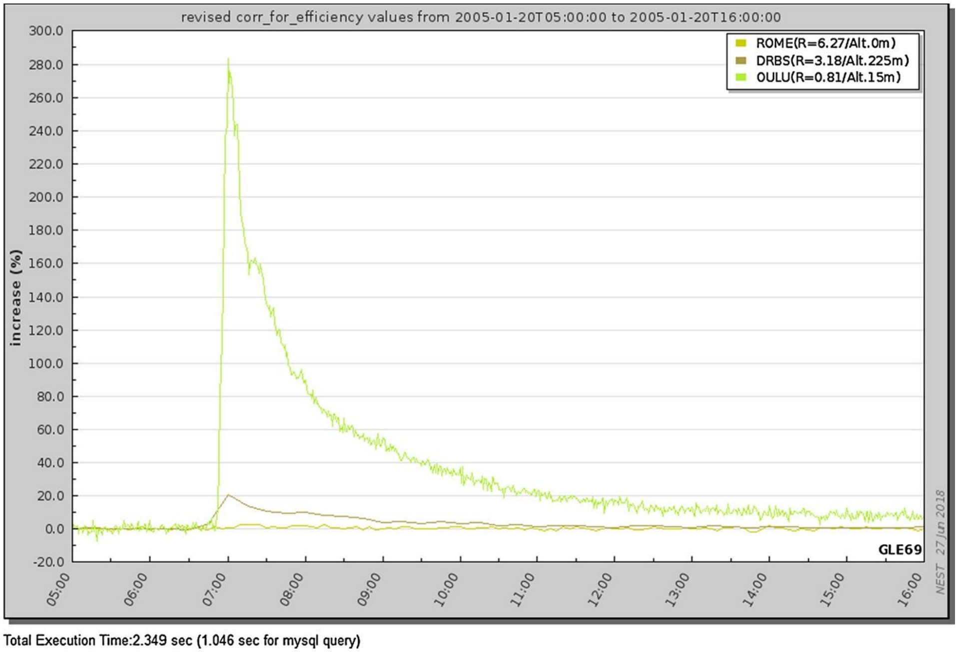

FIG. 20.8 A record of a ground level enhancement, the GLE #69 event that occurred on 20 January 2005 (data from Rome, Oulu, and Dourbes neutron monitors; image courtesy of NMDB).

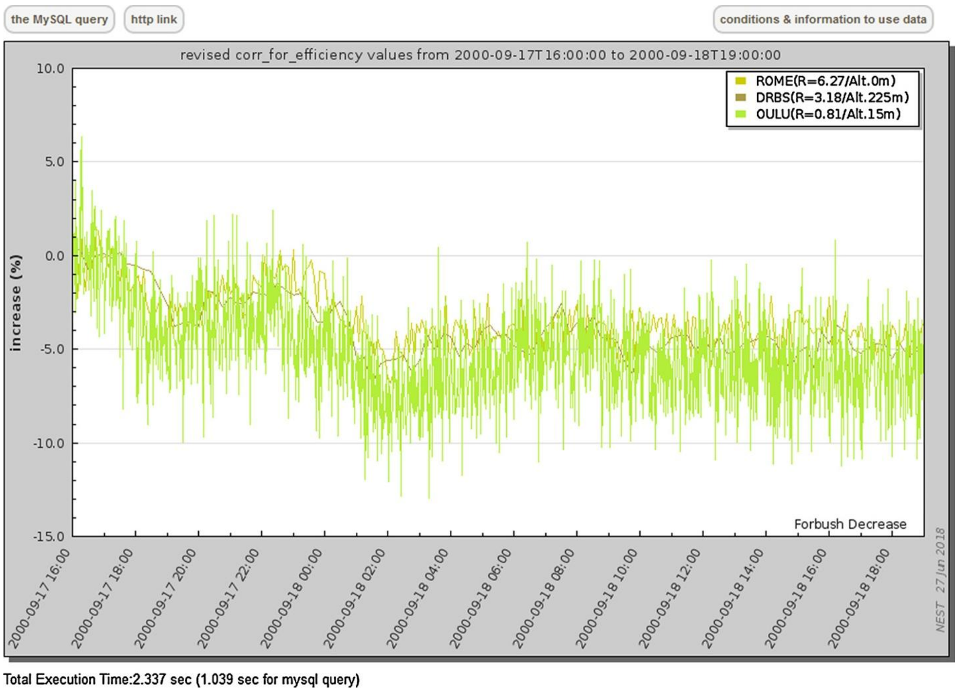

FIG. 20.9 A record of a Forbush decrease, the FD #39 event that occurred on 18 September 2000 (data from Rome, Oulu, and Dourbes neutron monitors; image courtesy of NMDB).

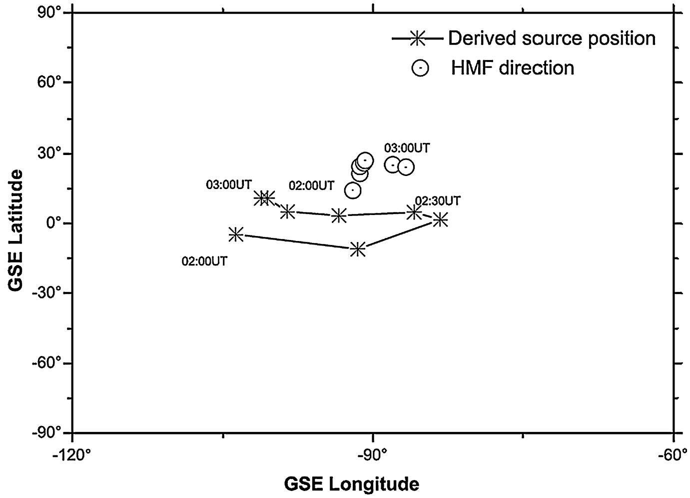

FIG. 20.10 Determination of the apparent source position and its evolution during GLE #71 (Geocentric Solar Ecliptic System) (Mishev et al., 2014) (copyright license No.: 4647560881398).

best results are obtained by calculating the yield function for every neutron monitor used for the analysis using the station-specific data parameters from the NMDB using any transport code (Ferrari et al., 2005; Allison et al., 2016). If data about the design parameters (dimensions and materials) of the station are not available, a more general yield function can be used (e.g., the yield function parametrized for atmospheric depth and rigidity proposed by Flückiger et al., 2008). Many yield functions are determined for specific conditions (sea level, specific solar activity, etc.). In this case the count rate of the different NMDB stations used for the analysis can be normalized to sea level using the 2-attenuation data correction (McCracken, 1962). With the yield function and a model of the solar particle spectrum, we can determine the apparent position of the solar particles and the pitch angle distribution (Debrunner and Lockwood, 1980). The data analysis is complex and requires additional measurements like the properties of the heliospheric magnetic field, the primary GCR spectra (from the GOES satellite), modeling of the atmospheric interactions, etc. The results of a detailed analysis of the GLE #71 from 17 May 2012 performed by Mishev et al. (2014) are illustrated in Figs. 20.10 and 20.11. The availability of high-resolution NMDB data allowed analyzing the progression of the GLE parameters and spectrum analysis like the evolution of the pitch angle during the different phases of the event (Fig. 20.12).

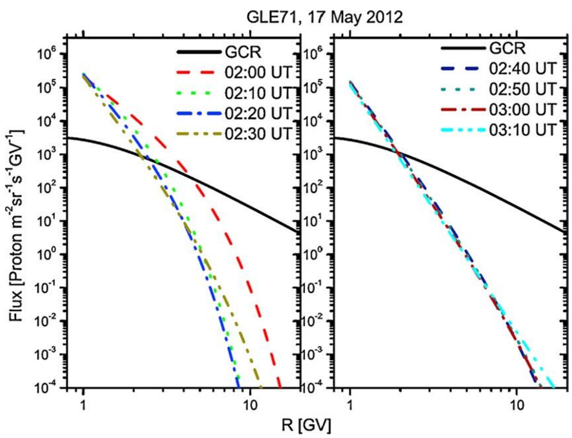

FIG. 20.11 GLE #71 analysis: high-energetic solar particle rigidity spectrum progression during the course of the GLE. The spectra are taken along the symmetry axis of the event (Mishev et al., 2014) (copyright license No.: 4647560881398).

20.3.2 Evaluation of the Radiation Effects on Electronics and Health

The neutron fluence at a given location can be determined. Neutrons in the energy range of 0.01–10 GeV may pose problems to the components of control electronics (airplanes, train traffic, automated cars, etc.) by single event effects (state flips between 0 or 1) (Gordon et al., 2004). A typical problem is the determination of the total neutron fluence during a ground-level en-

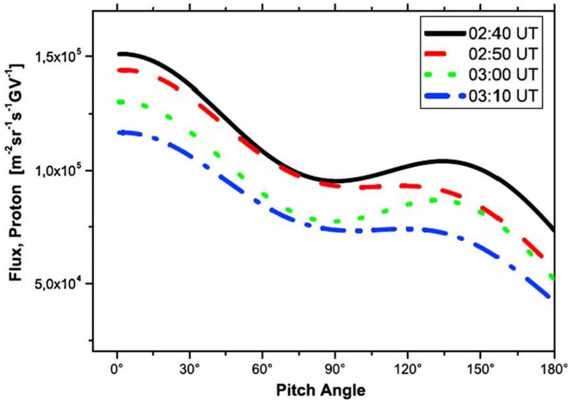

FIG. 20.12 GLE #71: Evolution of the primary particle pitch-angle distribution (Mishev et al., 2014) (copyright license No.: 4647560881398).

hancement event in the vicinity of a neutron monitor station. In this case, the count rate of the neutron monitor has to be corrected for multiplicity (i.e., the number of secondary neutrons produced per primary neutron within the neutron monitor) and for efficiency. The final fluence is then obtained by integration over the continuation of the GLE (work in progress). The results from the GLE analysis can be used to calculate the radiation doses at flight altitudes during a GLE event. The contribution of the GCRs to the effective dose rates was studied during the first space flights and the following missions. The modeling of the GCR spectrum is still under study and affects the results from the calculations of the radiation burden in space (Mrigakshi et al., 2013). The dose rate due to GCRs depends on the solar modulation and the geomagnetic latitude. A typical dose rate due to GCR during a flight between Europe and North America amounts to about 5 μSv/h (Matthiä et al., 2014). The contribution to this dose can be significant during a strong solar particle event (Reitz, 1993; Vainio et al., 2009). An extreme event may result in dose rates of about 3 mSv as calculated for the GLE #05 (Lantos and Fuller, 2004), which is about 3 times the annual occupational dose of 1 mSv. The high resolution data from NMDB allows determining the dose rates and their evolution due to solar energetic particles for a given location (i.e., flight path). The advantage of the NMDB data is that the anisotropies in the dose rates can be determined. For example, the analysis of Mishev et al. (2015) reported dose rates of 150 μSv/h over the North polar region and 1000 μSv/h over the South polar region during the main phase of GLE #69. The calculated dose rates depend on the methods used during the characterization of the GLE. This can introduce differences in the obtained results, as pointed out by Bütikofer and Flückiger (2013).

20.3.3 Space Weather Nowcast and Forecast

After collecting the available historical data from the neutron monitors world-wide and creating the infrastructure of registering and receiving data from high- and low-latitude stations in near-real-time, the efforts were focused on utilizing these data for characterization of the interplanetary space at the present moment (nowcast) and for prediction of possible GLE or SEP events (forecast). Space weather nowcast is possible because the GCRs occupy the interplanetary medium. Changes in the solar activity influence the interplanetary space and therefore the omnipresent GCRs (Kudela et al., 2000; Kudela and Storini, 2006). Hence by monitoring the cosmic rays intensity worldwide we can obtain information about the state of the solar activity. The first systematic and continuous space weather monitoring was the mininetwork of cosmic ray observatories Spaceship Earth, operated by the Bartol University (Bieber et al., 2004). The NMDB has many more stations, providing the opportunity for better evaluation of the current interplanetary conditions. A powerful tool for nowcasting is the evaluation of the cosmic ray anisotropies which are directly related to fluctuations in the interplanetary state (Asipenka et al., 2009; Eroshenko et al., 2009). Geomagnetic storms are also detected by the NMDB. The changes in the local geomagnetic field affect the geomagnetic cutoff rigidity and hence the count rate of the neutron monitor located at this point (Kudela and Bucik, 2005; Kudela and Usoskin, 2004). Changes in the relative intensity of a neutron monitor can be due to energetic solar particles, or a depreciation of the GCR flux due to propagating disturbances which sweep the GCRs, resulting in a decrease in the measured intensity. Solar particles contribute very little to the total flux and cannot be detected by satellites (Dorman et al., 2004). Analysis of such disturbances have pointed out that they result in specific changes of the count rate in the network of neutron monitors called precursors. They can manifest themselves as increase or decrease in the count rate before the arrival of the main phase of the disturbance (Belov et al., 2001, 2003, 2016). These observations have been quantified by Dorman et al. (2004) for utilizing the NMDB real-time measurements for forecasting of GLE occurrences. The GLE alert systems utilizing the NMDB data often run their own mirror of the database to allow a quick access to the available measurements

(IZMIRAN,[3] ANEMOS[4]) (Mavromichalaki et al., 2005; Kuwabara et al., 2006).

20.4 SUMMARY AND OUTLOOK

The main outlook for the future of NMDB is to improve the data availability for real-time applications. The time interval between the measurement and the arrival of the data to the database varies for the different remote stations with slow network infrastructure. The second important target is the improvement of the data quality. Many stations are still not checking basic data (e.g., out of range pressure measurements, noisy spikes in the intensity data, etc.). Cosmic rays are a formidable source of information about the universe and are still an important topic of international research, with many open questions waiting for answer, e.g., under what circumstances and how the charged particles are accelerated to such high energies or speeds. Modern applications frequently employ extensive arrays of monitors. In effect, the observing instrument is not an isolated instrument, but rather an array of instruments. Networking the neutron monitors yields new information in several areas, such as anisotropy, energy spectrum, relativistic solar neutrons, etc.

ACKNOWLEDGMENTS

The NMDB and the research results from the data provided by it received funding from the European Union's Seventh Framework Program, FP7 (2007–2013) under grant agreement No. 213007. Data retrieved via NMDB are the property of the individual data providers. We acknowledge the Rome, Oulu and Dourbes neutron monitors for providing data. The authors thank Dr. Christian Steigies for the helpful discussions.

REFERENCES

Allison, J., Amako, K., Apostolakis, J., et al., 2016. Recent developments in Geant4. Nuclear Instruments & Methods in Physics Research. Section A, Accelerators, Spectrometers, Detectors and Associated Equipment 835, 186–225.

Asipenka, A., Belov, A., Eroshenko, E., et al., 2009. Asymptotic longitudinal distribution of cosmic ray variations in real time as the method of interplanetary space diagnostic. In: Proc. 31st International Cosmic Rays Conference, Lòdž 2009 (ICRC 2009), p. 2.

Belov, A.V., Abunina, M.A., Abunin, A.A., et al., 2017. Vector anisotropy of cosmic rays in the beginning of Forbush effects. Geomagnetism and Aeronomy 57, 541–548.

Belov, A.V., Bieber, J.W., Eroshenko, E.A., et al., 2001. Pitch-Angle features in cosmic rays in advance of severe magnetic storms: neutron monitor observations. In: International Cosmic Ray Conference, vol. 9, p. 3507.

Belov, A.V., Bieber, J.W., Eroshenko, E.A., et al., 2003. Cosmic ray anisotropy before and during the passage of major solar wind disturbances. Advances in Space Research 31, 919–924.

Belov, A.V., Eroshenko, E.A., Abunina, M.A., et al., 2016. Behavior of the cosmic ray density during the initial phase of the Forbush effect. Geomagnetism and Aeronomy 56, 645–651.

Bieber, J.W., Evenson, P., Dröge, W., et al., 2004. Spaceship Earth observations of the Easter 2001 solar particle event. The Astrophysical Journal Letters 601 (1), L103–L106.

Bütikofer, R., Flückiger, E.O., 2013. Differences in published characteristics of GLE60 and their consequences on computed radiation dose rates along selected flight paths. Journal of Physics. Conference Series 409, 012166.

Caballero-Lopez, R.A., Moraal, H., 2012. Cosmic-ray yield and response functions in the atmosphere. Journal of Geophysical Research: Space Physics 117 (A12), 103.

Clem, John M., Dorman, Lev I., 2000. Neutron monitor response functions. Space Science Reviews 93 (1), 335–359.

Debrunner, H., Lockwood, J.A., 1980. The spatial anisotropy, rigidity spectrum, and propagation characteristics of the relativistic solar particles during the event on May 7, 1978. Journal of Geophysical Research 85, 6853–6860.

Dorman, L.I., Pustilnik, L.A., Sternlieb, A., et al., 2004. Monitoring and forecasting of great solar proton events using the neutron monitor network in real time. IEEE Transactions on Plasma Science 32 (4), 1478–1488.

Eroshenko, E., Asipenka, A., Belov, A., et al., 2009. Definition of cosmic ray density and anisotropy vector beyond the magnetosphere in real time mode. In: Proc. 31st International Cosmic Rays Conference, Lòdž 2009 (ICRC 2009), p. 2.

Ferrari, A., Sala, P.R., Fassò, A., Ranft, J., 2005. FLUKA: a multi-particle transport code. Technical Report INFN/TC_05/11, SLAC-R-773. CERN.

Flückiger, E.O., Moser, M.R., Pirard, B., Bütikofer, R., Desorgher, L., 2008. A parameterized neutron monitor yield function for space weather applications. In: International Cosmic Ray Conference, vol. 1, pp. 289–292.

Forbush, S.E., 1946. Three unusual cosmic-ray increases possibly due to charged particles from the Sun. Physical Review 70, 771–772.

Gordon, M.S., Goldhagen, P., Rodbell, K.P., et al., 2004. Measurement of the flux and energy spectrum of cosmic-ray induced neutrons on the ground. IEEE Transactions on Nuclear Science 51 (6), 3427–3434.

Hatton, C.J., Carimichael, H., 1964. Experimental investigation of the NM-64 neutron monitor. Canadian Journal of Physics 42, 2443–2472.

Kudela, K., Bucik, R., 2005. Low energy cosmic rays and the disturbed magnetosphere. In: Solar Extreme Events: Fundamental Science and Applied Aspects (SEE-2005), International Symposium. Nor Amberd, Armenia, 26–30 September, 2005.

[3] http://cr0.izmiran.ru/GLE-AlertAndProfilesPrognosing/.
[4] http://cosray.phys.uoa.gr/index.php/glealertplus.

Kudela, K., Mavromichalaki, H., Papaioannou, A., Gerontidou, M., 2009. On mid-term periodicities in cosmic rays: utilizing the NMDB archive. In: Proc. 31st International Cosmic Rays Conference, Lòdż 2009 (ICRC 2009), p. 2.

Kudela, K., Storini, M., 2006. Possible tools for space weather issues from cosmic ray continuous records. Advances in Space Research 37, 1443–1449.

Kudela, K., Storini, M., Hofer, M.Y., Belov, A., 2000. Cosmic rays in relation to space weather. Space Science Reviews 93, 153–174.

Kudela, K., Usoskin, I.G., 2004. On magnetospheric transmissivity of cosmic rays. Czechoslovak Journal of Physics 54, 239–254.

Kuwabara, T., Bieber, J.W., Clem, J., Evenson, P., Pyle, R., 2006. Development of a ground level enhancement alarm system based upon neutron monitors. Space Weather 4 (10).

Lantos, P., Fuller, N., 2004. Semi-empirical model to calculate potential radiation exposure on board airplane during solar particle events. IEEE Transactions on Plasma Science 32, 1468–1477.

Lockwood, J.A., Webber, W.R., 1967. Differential response and specific yield functions of cosmic-ray neutron monitors. Journal of Geophysical Research 72, 3395–3402.

Matthiä, D., Meier, M.M., Reitz, G., 2014. Numerical calculation of the radiation exposure from galactic cosmic rays at aviation altitudes with the PANDOCA core model. Space Weather 12, 161–171.

Mavromichalaki, H., Gerontidou, M., Mariatos, G., et al., 2005. Space weather forecasting at the new Athens center: the recent extreme events of January 2005. IEEE Transactions on Nuclear Science 52, 2307–2312.

Mavromichalaki, H., Papaioannou, A., Plainaki, C., et al., 2011. Applications and usage of the real-time Neutron Monitor Database. Advances in Space Research 47, 2210–2222.

McCracken, K.G., 1962. The cosmic-ray flare effect: 1. Some new methods of analysis. Journal of Geophysical Research 67 (2), 423–434.

Mishev, A.L., Adibpour, F., Usoskin, I.G., Felsberger, E., 2015. Computation of dose rate at flight altitudes during ground level enhancements no. 69, 70 and 71. Advances in Space Research 55 (1), 354–362.

Mishev, A.L., Kocharov, L.G., Usoskin, I.G., 2014. Analysis of the ground level enhancement on 17 May 2012 using data from the global neutron monitor network. Journal of Geophysical Research: Space Physics 119, 670–679.

Mishev, A.L., Usoskin, I.G., Kovaltsov, G.A., 2013. Neutron monitor yield function: new improved computations. Journal of Geophysical Research: Space Physics 118, 2783–2788.

Mrigakshi, A.I., Matthiä, D., Berger, T., Reitz, G., Wimmer-Schweingruber, R.F., 2013. How Galactic Cosmic Ray models affect the estimation of radiation exposure in space. Advances in Space Research 51, 825–834.

Reitz, G., 1993. Radiation environment in the stratosphere. Radiation Protection Dosimetry 48 (1), 5–20.

Sapundjiev, D., Nemry, M., Stankov, S., Jodogne, J.C., 2014. Data reduction and correction algorithm for digital real-time processing of cosmic ray measurements: NM64 monitoring at Dourbes. Advances in Space Research 53 (1), 71–76.

Sapundjiev, D., Stankov, S., Jodogne, J.C., 2016a. Present status and modernisation of the Dourbes cosmic ray observatory for improved space weather research and forecasting. In: Proc. European Space Weather Week (ESWW). 14–18 November 2016, Ostende, Belgium.

Sapundjiev, D., Steigies, C., Verhulst, T., Jodogne, J.C., Stankov, S., 2016b. Upgrading the Dourbes cosmic ray observatory for research and development of improved space weather monitoring services. In: Proc. European Space Weather Week (ESWW). 23–27 November 2015, Ostende, Belgium.

Simpson, J.A., 2000. The cosmic ray nucleonic component: the invention and scientific uses of the neutron monitor. Space Science Reviews 93 (1), 11–32. IGY neutron monitor development.

Simpson, J.A., Fonger, W., Treiman, S.B., 1953. Cosmic radiation intensity-time variations and their origin. I. Neutron intensity variation method and meteorological factors. Physical Review 90, 934–950.

Steigies, C.T., for the NMDB Consortium, 2016. The Neutron Monitor Database (NMDB) and its applications to space weather. Workshop on cosmic rays and space weather: research activities, service developments, and future strategy. Dourbes, Belgium, https://events.spacepole.be/event/10/sessions/4/attachments/11/60/03-nmdb.pdf.

Steigies, C.T., Klein, K.L., Fuller, N., NMDB Consortium, 2009. www.nmdb.eu: the real-time neutron monitor database. In: Proc. 31st International Cosmic Rays Conference, Lòdż 2009 (ICRC 2009), p. 2.

Stoker, P.H., 2009. The IGY and beyond: a brief history of ground-based cosmic-ray detectors. Advances in Space Research 44, 1081–1095.

Treiman, S.B., 1952. Analysis of the nucleonic component based on neutron latitude variations. Physical Review 86, 917–923.

Vainio, R., Desorgher, L., Heynderickx, D., et al., 2009. Dynamics of the Earth's particle radiation environment. Space Science Reviews 147 (3–4), 187–231.

Wainio, K.M., Colvin, T.H., More, K.A., Tiffany, O.L., 1968. Calculated specific yield functions for neutron monitors. Canadian Journal of Physics 46 (10), S1048–S1051.